Journal of Membrane Science & Research

journal homepage: www.msrjournal.com

Research Paper

A Novel Polymer Inclusion Membrane Containing an Organometallic Complex Carrier for The Extraction and Recovery of Chromium and Nickel from Wastewater

Zakaria Habibi [1], Chaouqi Youssef [1,2,*], Mohammed Riri [1], Sanaa Majid [1], Khalifa Touaj [1], Miloudi Hlaibi [1]

[1] *Laboratory of Materials Engineering for Environment and Valorization (GeMEV), Faculty of Sciences Chock, University Hassan II, Casablanca, Morocco*
[2] *Laboratory of Research on Textile Materials (REMTEX), ESITH Casablanca, Morocco*

Article info

Received 2022-05-20
Revised 2022-09-02
Accepted 2022-09-16
Available online 2022-09-16

Keywords

Affinity polymer membranes
Permeability
Extraction process
Initial flux
Selective separation of Cr(VI) and Ni (II) ions

Highlights

- Development and characterization of novel polymer inclusion membranes (PIMs).
- The interpretation of all the parameters approved for the explants results obtained.
- Selectively extracting Cr (VI) and Ni (II) from industrial solutions is possible.

Graphical abstract

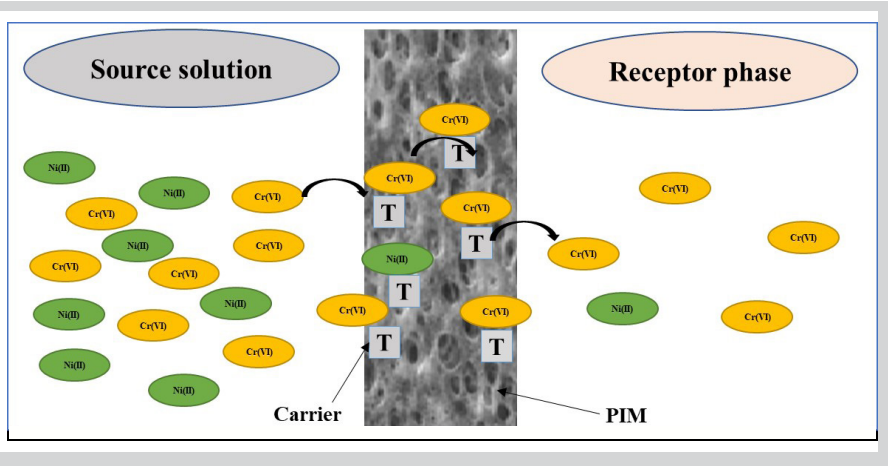

Abstract

In this study, two types of affinity polymer membranes containing new organometallic complexes (Gd-glucaric acid) as extractants were prepared and characterized. They were used to extract Cr (VI) ions from concentrated solutions (0.0068M–0.0009 M). These affinity polymer membranes were tested by designing an easier extraction process from the substrate at different concentrations and different temperatures. Additionally, macroscopic parameters such as permeability (P) and initial flux (J_0) were evaluated to explain the extraction process of the substrate using these membranes. The results showed that the value of the initial flux (J_0) of the extracted substrate was related to its initial concentration C_0 by the saturation law, which allowed determining the microscopic parameters, the apparent diffusion coefficient (D^*), and the substance formed (substrate-extraction agent) along with its constant correlation (K_{ass}). The substrate factors and the temperature significantly affected the evolution of these parameters and the performance of the membrane during extraction. The activation parameters (E_a, $\Delta H^{\neq}$, and $\Delta S^{\neq}$) were determined, and the results indicated that the high performance of these types of membranes is related to the use of advanced techniques. The efficiency was related to the movement properties of the substrate through the organic phase and the structure of the membrane. The membranes developed were used to conduct experiments related to selective extraction and removal of chromium ions from a mixture containing Ni (II) ions. The results of these tests were conclusive and indicated a co-transport of Cr (VI) and Ni (II) ions, along with a marked reduction in the values of P and J_0, which enhanced the performance of the membrane.

1. Introduction

The textile industry consumes the largest quantity of water among all types of industries. Specifically, the dyeing and finishing phases mainly use chemicals that are harmful to health and cause pollution of surface water and groundwater [1]. Mordant dyes used in these industries are a source of metallic

* Corresponding author: chaouqi.youssef@gmail.com (C. Youssef)

DOI: 10.22079/JMSR.2022.546447.1527

pollution since they usually contain functional ligands that react strongly with Chromium(VI), Copper(II), Nickel(II), and Cobalt(II), producing complexes of different colors with the textile [2]. The wastewater resulting from the dyeing, finishing, and rinsing phases of dyed textile fibers contains large quantities of dyes and traces of metals such as Chromium(VI), Nickel(II), Cobalt(II), and Copper(II) ions [3].

Metallic ions, especially heavy metals, are the most dangerous water pollutants. The heavy metals that are naturally present in the environment, are among the most toxic pollutants [4]. Therefore, treating textile effluents is necessary before discharging them into the aquatic systems [5]. Their impact on the environment occurs not only due to their strong toxicity that damages the aquatic environment but also due to their accumulation throughout the food chain which directly threatens the health of organisms [6]. To reduce the abundance of metal ions in the environment, several processes have been used for removing and recovering ions from textile effluents, including liquid-liquid extraction [7], ion exchange processes [8] chemical precipitation [9,10], and membrane processes [11,12].

Membrane processes are used in many industrial applications, either to recover or separate the constituents of a mixture or selectively control the exchange of matter between different media [13]. The application of membrane techniques has grown rapidly in recent years, mainly due to its ever-growing applications in various fields. Membranes are promising due to their low error forecast. After establishing their utility in the fields of industry and health [14], their applications are now being extended to the fields of environment and advanced technologies.

Membrane technology has many advantages and many uses. These processes are clean, more ecological, and more efficient than alternatives to conventional methods of wastewater treatment. Membrane processes can remove heavy metal ions, such as Cr (VI) ions. Different types of membranes can be used for removing Cr(VI) ions, such as inorganic film membranes [15,16], polymers [17,18], and liquid membranes [17,19].

Polymer inclusion membranes (PIMs) are more stable and efficient, especially compared to other liquid membranes. They usually consist of a polymer carrier, an extractant, plasticizers, or porosity modifiers. The exacting agent is a complex-forming agent or ion exchanger responsible for interacting with target species and their propagation to the stage of the PIM. Many types of acidic, basic, neutral amphiphilic agents, and macromolecular solvents, are used to accurately and efficiently transport and separate Cr (VI) ions from aqueous solutions [20,21]. New polymer inclusion membranes can be used to recover Chromium and Nickel from textile wastewater containing NTA as a carrier [22].

In this study, we used the membrane separation processes to facilitate the separation and extraction of Cr (VI) ions from an aqueous solution. Thus, we focused on the development of two PIMs based on two polymer supports, i.e., (PVDF+PVP) and (PSU+PVP). A new extractive agent (EA), gadolinium-glucaric acid complex, was also used in the process. Additionally, to study the performance of the developed PIMs, we determined the macroscopic parameters (membrane permeability P and initial flux J_0) and microscopic parameters (the association constant K_{ass} and the apparent diffusion coefficient D*) based on Fick's first law and the saturation law of the extractant agent by the substrate(S). Moreover, to account for the recovery of the substrate Cr (VI) performed by the membrane, and elucidate the mechanistic aspects, the activation parameters, E_a energy, enthalpy $\Delta H^{\neq}$, and entropy $\Delta S^{\neq}$, were determined. The yields obtained with different PIMs for the recuperation and separation of Cr (VI) were compared. Additionally, the effect of factors such as temperature and concentration on the removal performance was also studied. The mechanism of selective separation of Cr (VI) from a mixture containing Ni (II) ions was elucidated.

2. Materials and Methods

2.1 Reagents

To synthesize PIMs, raw materials for the synthesis of new extractants, such as the Gd-glucaric acid complex, were purchased from Sigma-Aldrich. The method used for preparing the polymer carrier is discussed in the following sections. Polyvinylidene fluoride (PVDF) (molecular weight 440,000 $gmol^{-1}$) was purchased from Alfa Aesar. Polysulfone (PSU) (molecular weight 35,000 $gmol^{-1}$) was purchased from Sigma-Aldrich, and Polyvinylpyrrolidone PVP (molecular weight 40,000 $gmol^{-1}$), was purchased from Alfa Aesar, a copolymer. Potassium dichromate [$K_2Cr_2O_7$] (molecular weight 294.185 $gmol^{-1}$) was purchased from Sigma-Aldrich. Substrate solutions of Cr (VI) or Ni (II) ions were prepared by dissolving the matrix in distilled water. Initially, $[Ni^{2+}]_0 = [Cr_2O_7^{2-}]_0 = C_0 = 2\ gL^{-1}$ was added to distilled water without adding any auxiliary compounds. Then, concentrated solutions of HCl and NaOH were used to regulate the pH of the solution. All chemicals, reagents, and solvents used in the experiment were commercial products.

2.2 Preparation of the extracting agent

The complex Gd-glucaric acid was synthesized following the protocol suggested in our laboratory by Riri et al. [23]. The solution was formed by mixing glucaric acid (ligand) and ($Gd(NO_3)_3.6H_2O$) at a concentration of 10^{-2} M and fixed pH. The complex was precipitated rapidly at room temperature (Fig. 1). And was insoluble in water, methanol, and ethanol.

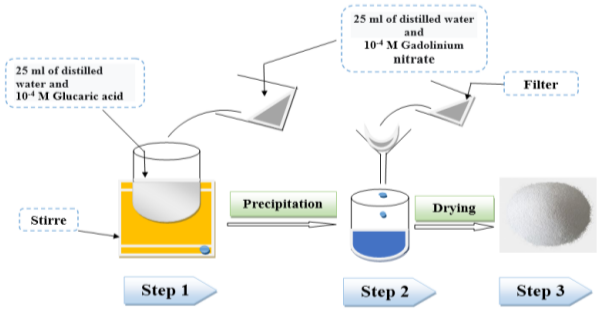

Fig. 1. Preparation of the complex

2.3 Membrane preparation

The polymer inclusion membranes were designed according to the following experimental protocol. First, 3 g of polysulfone (PSU) or polyvinylidene fluoride (PVDF was dissolved in 12.5 mL of DMF at room temperature and stirred continuously for 12 h, Then 0.6 g of polyvinylpyrrolidone (PVP) was added. To this mixture, a fixed amount of the Gd-glucaric acid complex carrier was added. It was then stirred for two days in the absence of air to completely solubilize the added complex. The paste obtained was poured and spread onto a glass plate, and the plate was immersed in a bath containing distilled water. The DMF solvent left the matrix of the spread paste, and a rigid membrane was obtained (Fig. 2) (Phase inversion method) [24,14].

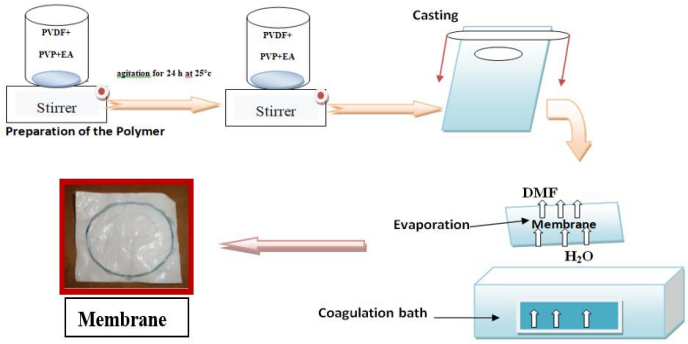

Fig. 2. Preparation of the PIM based on the phase inversion method

Two membranes containing organometallic complexing agents were developed including PIM (1): PVDF + PVP + Glucaric acid and PIM (2): PSU + PVP+ Complex (Gd-glucaric acid). The thickness of the prepared membrane was measured using the Mitutoyo Electronic Palmer (Mitutoyo Co., Ltd., Takatsu District, Kawasaki City, Kanagawa Prefecture, Japan), and the accuracy was found to be±0.002 mm. It was then isolated from air and stirred for two days to completely solubilize the added complex. The cell used to conduct the experiments associated with the facilitated transport of Cr (VI) or Ni (II) ions consisted of two glass compartments separated by the prepared membrane. One compartment contained the source solution of the metal ion at the studied concentration, and another compartment contained the receptor phase. The system was immersed in a thermostat bath containing water to keep the temperature constant throughout the experiment. A multi-stage stirrer was used to ensure the homogeneity of the two phases (Fig. 3).

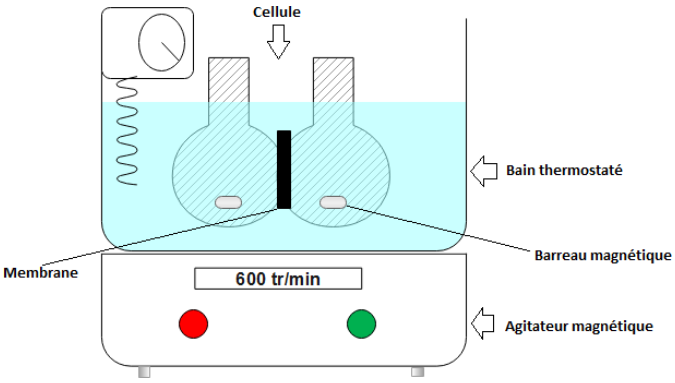

Fig. 3. Transport cell.

3. Theoretical calculations

3.1 Kinetic model to calculate the macroscopic parameters P and J_0

The kinetic model developed by Verchère in the PBS laboratory in Rouen was used in this study. The reliability of this model was reassured by using it in several other studies in our laboratory [25,26].

The membrane was placed between the two glass compartments of the transport cell. A known volume of the substrate solution at C_0 concentration was placed in the source compartment (S). Several samples were taken at regular time intervals (30 min) from the receptor phase R to follow the evolution of the concentration of this receptor phase in the substrate (Cr(VI)). Assuming C_R to be the concentration of the substrate in the receptor phase at each instant, the concentration in the source phase can be expressed as $C_F = C_0 - C_R$.

The relationship between the flux J of the substrate and its concentration is:

$$dCR/dt = J \times S/V \quad (1)$$

Where S is the surface area of the membrane, V is the volume of the receiving phase, and J is the flux.

The relationship of flux J with ΔC (the difference between the substrate concentration in the source (C_F) and receptor (C_R) phases) and the membrane thickness E is shown in equation (2) derived from Fick's First Law.

$$J = P \times \frac{\Delta C}{E} \quad (2)$$

P denotes the permeability of the membrane.

$$C_F = C_0 - C_R \text{ thus, } \Delta C = C_F - C_R = C_0 - 2C_R \quad (3)$$

Where C_0 is the initial concentration of the solute in the source phase C_F is the concentration of the solute in the source phase.

By combining equations (1), (2), and (3), the following differential equation was obtained:

$$P \times dt = (E \times V/S)\, dC_R/(C_0 - 2\,C_R) \quad (4)$$

The integration of equation (4) gives:

$$P \times (t - t_l) = (E \times V/S)\,[1/2Ln\,(C_0/(C_0 - 2\,C_R)] \quad (5)$$

The equation showed that after an induction period, which can be several hours, the term

-Ln (C_o-2C_R) becomes a linear function of time t.

$$P = a \times V \times E/2S \quad (6)$$

Here a denotes the slope used to calculate the permeability P.

The initial flow J_0 can be calculated from the permeability P according to the following equation

$$J_0 = P \times C_0/E \quad (7)$$

The end of the manipulation corresponded to a dynamic equilibrium, which was established between the two compartments ($C_F = C_R = C_0/2$), and the diffusion velocities in the two directions became equal.

*3.2 Theoretical model to determine the microscopic parameters K_{ass} and D**

Transport depends on the formation and dissociation of the substrate-transporter (ST) complex at the solution-membrane interface. The transporter (T) is insoluble in water, and the substrate is insoluble in the membrane.

The complexation equilibrium can be expressed as,

T (org) + S(aq) ⟷ TS (org)

$$[TS]i = Kass \times [T]i \times [S]i \text{ (laws of mass action)} \quad (8)$$

where K_{ass} is the Formation constant of the TS complex, $[S]_t$ is the Substrate concentration at time t in the source phase and at the substrate/membrane interfaces, $[S]_i$ is the Substrate concentration at the interface, $[T]_i$ is the Carrier concentration at the interface, and $[TS]_i$ is the Complex (T-S) concentration at the interface.

According to Fick's law, substrate flux is proportional to the concentration of the complex in the membrane and can be expressed as,

$$J = (D/E) \times [TS] \quad (9)$$

where D is the apparent diffusion coefficient and E is the thickness of the membrane.

However, at the interface, on the source phase side $[TS]_i << [S]_i$, and the substrate concentration $[S]_i$ is equal to that of the substrate at time $[S]_t$ ($[S]_i = [S]_t$).

The total concentration $[T]_0$ of the transporter immobilized on the membrane is constant. It is equal to the sum of the concentrations $[T]_i$ and $[TS]_i$

$$[T]_0 = [T]_i + [TS]_i = [T]_i \times (1 + K_{ass} \times [S]_i) \quad (10)$$

$$[T]i = [T]_0/(1 + K_{ass} \times [S]_i) = [T]_0/(1 + K_{ass} \times [S]_t) \quad (11)$$

In the initial conditions, $J_0 = (D/E) \times K_{ass} \times [T]_i \times [S]_t$ function of $[T]_0$ and C_0.

$$J_0 = \{(D/E) \times K_{ass} \times [T]_0 \times C_0\}/(1 + K_{ass} \times C_0) \quad (12)$$

This expression is used to calculate the permeability P as a function of $[T]_0$ and C_0: $P = J_0 \times E/C_0$

$$P = D \times K_{ass} \times [T]_0/(1 + K_{ass} \times C_0) \quad (13)$$

J_0 and P were proportional to the initial carrier concentration. These expressions suggested Michaelis-Menten-type transport law since carrier saturation was observed at high values of C_0.

For determining the apparent diffusion coefficient D* and the association constant K_{ass} of the complex (substrate-carrier), the Lineweaver-Burk line was drawn for the flux:

$$1/J_0 = f\,(1/C_0) = (E/D) \times \{(1/[T]_0 \times K_{ass}) \times (1/C_0) + (1/[T]_0)\} \quad (14)$$

Here,

$$K_{ass} = intercept\ (oo)/slope\ (p) \text{ and } D^* = (1/oo) \times (1/[T]_0) \quad (15)$$

The initial flow was related to the temperature by the Arrhenius law as follows:

$$J(T) = A_j\, exp\,(-E_a/RT) \quad (16)$$

Here, R denotes the perfect gas constant, A_j denotes the pre-exponential factor, and E_a denotes the activation energy for the formation of the transition state relative to the kinetically determining step, which is the diffusion of the complex (T-S) through the membrane [27-29].

After linearization, equation (15) be expressed as:

$$lnJ_0 = -E_a/R \times (1/T) + lnA_j \quad (17)$$

E_a can be calculated from the slope of the curve ln J_0 = f(1/T).

The activated complex theory suggests that E_a is related to the enthalpy of activation $\Delta H^\sharp$ by the equation

$$\Delta H^\sharp = E_a - 2500\ (J/mol)\ at\ 25\ °C \quad (18)$$

While the entropy $\Delta S^\sharp$ is linked to the pre-exponential factor by the equation,

$$\Delta S^\sharp = R\ (lnA_j - 30.46)\ at\ 25\ °C \quad (19)$$

4. Results and discussion

4.1 Characterization of the PVDF+PVP/PVDF+PVP+Complex membranes and PSU+PVP/PSU+PVP+Complex by FTIR

To confirm the presence of a carrier in the developed membranes, the FTIR spectra of the membrane containing the PVDF + PVP support polymer were compared to the PVDF+ PVP/complex membrane. The peaks observed in the spectrum of the membrane containing PVDF and PVP were characterized by a band at 1404 cm^{-1}, which might be attributed to the CH groups. Similarly, bands at 876 cm^{-1}, and those occurring between 1074 and 1278 cm^{-1} correspond to the vibration of the linear C-C bond and the elongation vibrations of the C-F bonds, respectively (Fig. 4). The spectrum of the PVDF-Complex membrane showed a band characteristic of the C=O and O-H groups present in the complex molecule, which indicated the integration of the carrier with the membrane.

The infrared spectrum of the PSU-PVP membrane **(**Fig. 5**)** showed the characteristic vibration band of the PSU polymer support. This might be related to the extension of the functional groups: O= S=O (1014 cm^{-1}), C-H (689/381 cm^{-1}), and C=C-C (1488/1585 cm^{-1}). The O-H and C=O functional groups showed characteristic vibration bands near 3350 and 1750 cm^{-1}, respectively. The spectrum of PSU+PVP-Complex showed the disappearance of the C=O band, which indicated the integration of the extraction molecule (Complex) with the support (PSU+PVP).

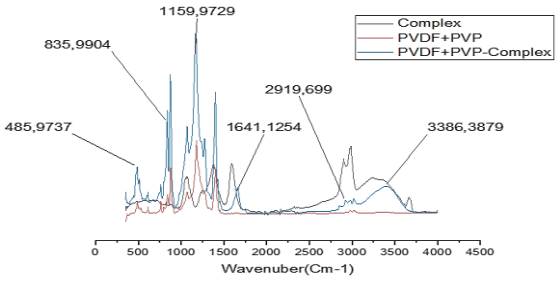

Fig. 4. The FT-IR spectra for the PVDF + PVP support and the PVDF+ PVP/complex membrane.

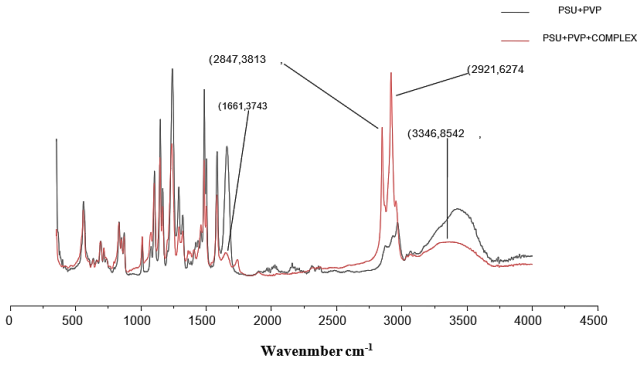

Fig. 5. The FT-IR spectra of the PSU + PVP support and the PSU + PVP/complex membrane

4.2 Characterization of the PVDF+PVP/PVDF+PVP+Complex membranes and PSU+PVP/PSU+PVP+complex by SEM

The SEM images of the surface and cross sections of the two developed PIMs are shown in Fig. 6 and 7. Differences were found between the membranes composed of the PVDF/PVP [11] and PSU/PVP [30], polymer supports only, and each membrane containing a transport agent. The images showed that the PVDF/PVP or PSU/PVP membranes were homogeneous with very smooth surfaces and sections. The addition of transporters to the PVDF/PVP or PSU/PVP polymer supports altered the membrane structure (morphology and porosity) (Fig. 6 and 7). The surface became porous, with relatively uniform pores. Cross-sectional images showed the presence of cavities of different sizes. Thus, depending on the nature and chemical structure of the extractant, the inclusion of a transport agent can facilitate the formation of pores of different sizes and shapes in the membrane.

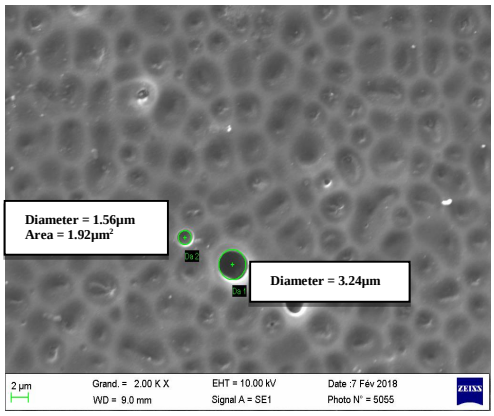

Fig. 6. SEM images of PVDF/PVP-Complex

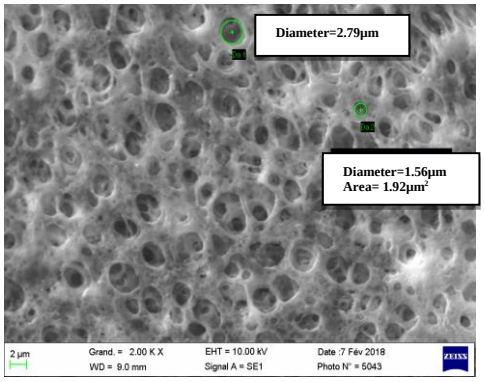

Fig. 7. SEM images of PSU/PVP-Complex.

4.3 Influence of the substrate (Cr (VI)) concentration

To determine the effect of the initial Cr (VI) concentration on the evolution of macroscopic parameters (initial flux J_0 and permeability P) and microscopic parameters (association constant K_{ass} and apparent diffusion coefficient D*), we performed facilitated transport through the two selected membranes, i.e., PIM(1) and PIM(2) under different Cr (VI) concentrations (0.0068, 0.0034M, 0.0017M, and 0.0009M) at pH=3 and T=25°C. We evaluated the parameters that played a crucial role in determining the facilitated extraction of Cr (VI) ions. While performing manipulations, the concentration of the Cr (VI) ion evolved in the receptor phase was recorded as a function of time and plotted for each of the studied membranes using the function-Ln (C_0–$2C_R$) =f (time) at different Cr (VI) ion concentrations **(**Fig. 8**)**.

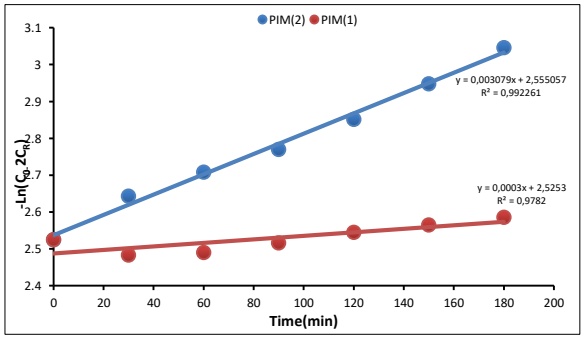

Fig. 8. Representation of the-Ln (C_0–$2C_R$) = f(t) lines of Cr (VI) ion transport through the two PIMs at pH=3 and T=25°C (Co=0.0068M).

The kinetic term, -Ln (C_0–$2C_R$) = f(t), was represented by straight lines, showing that the transport of the Cr (VI)ions across these membranes fit well with the proposed kinetic model. The model considered the diffusion of the carrier-substrate complex across the membrane to be the rate-determining step.

From the slopes of these lines, we determined the macroscopic parameters (P and J_0) related to the directed process of facilitated Cr (VI) ion transport across the membranes for the concentrations studied. The results are presented in Table 1.

The permeability of the two membranes increased when the concentration of Cr (VI) in the source phase decreased (Table 1). The initial flux varied in the opposite direction, i.e., it increased with an increase in C_0. New polymer inclusion membranes were used for recovering chromium and nickel from textile wastewater using NTA as a carrier Overall, comparing the parameters of the two membranes, we found that PIM(2) was a more permeable membrane for the Cr(VI) ion substrate with permeability and initial flow approximately three times greater than the PIM(1)membrane. This was mainly because, in PIM(2), the molecules of the transporter were free in the membrane matrix, which favored the right structural orientations, and facilitated the association between the molecules of the transporter and those of the substrate Cr(VI) [31].

4.4 Influence of temperature

The process was conducted at different temperatures (25, 30, and 35 °C) to determine the effect of temperature on the evolution of the parameters of Cr (VI) ion transport through the membranes. For this, we fixed the other experimental conditions. The pH was set to 3 and we used the same agitation, the same volume of the two phases, and the same concentration of the substrate. The lines corresponding to-Ln(C_0-2C_R)= f(time)) were drawn in the same way and could be used to deduce the values of the macroscopic parameters related to the facilitated extraction of the Cr (VI) ions **(**Table 2**).**

These results suggested that for a given substrate concentration, the permeability of the membrane increased with temperature. A similar trend was also observed for the initial flux J_0 The parameters of PIM (2) were more important than those of PIM (1).

To determine the effect of temperature on the evolution of the microscopic parameters (apparent diffusion coefficient D* and the association constant K_{ass}) related to the facilitated extraction of Cr (VI) ions through the two membranes (PIM(1) and PIM(2)), we plotted the Lineweaver-Burk representations for each of the membranes at different temperatures (Fig. 9).

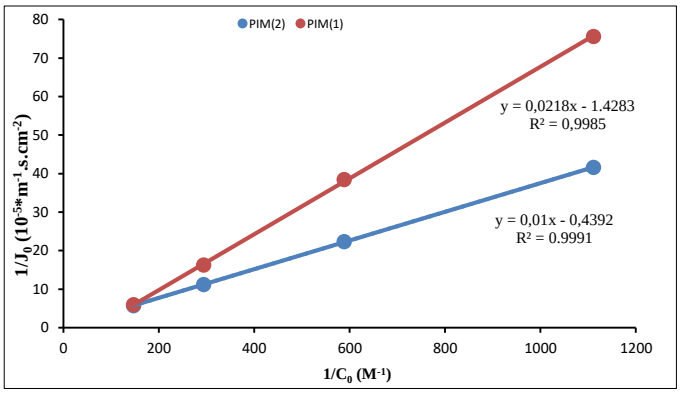

Fig. 9. The Lineweaver-Burk representation for the facilitated transport of Cr(VI) ions across the two membranes

From the slopes and intercepts of these lines, the microscopic parameters related to the facilitated transport of Cr (VI) ions for the two membranes at specific temperatures were determined and the results are shown in Table 3.

These results showed that an increase in the temperature caused a substantial increase in the apparent diffusion coefficient D* but only a slight decrease in the association constant K_{ass} for the two membranes. This might be due to an increase in the system energy, which favored the mobility of the molecules of the carrier and those of the Cr (VI) ions inside the membrane matrix, facilitating the structural orientations for fast and simple association/dissociation of the substrate with the carrier.

Table 1
Macroscopic parameters related to the process of facilitated transport of Cr(VI) ions.

Concentration C_0 (M)	PIM(2)		PIM(1)	
	P*10^7 cm^2 /s	$J_0 \times 10^5$ mmol/s.cm^2	P*10^7 cm^2 /s	$J_0 \times 10^5$ mmol/s.cm^2
0.0068	27.71	0.19	72.91	0.49
0.0034	28.17	0.15	80.21	0.27
0.0017	29.35	0.05	87.50	0.15
0.0009	31.08	0.03	94.79	0.08

Table 2
Influence of temperature on the macroscopic parameters of facilitated Cr(VI) ion transport across two membranes.

T(°C)	C_0 (M)	PIM (1)		PIM (2)	
		P*10^7 (cm^2 s^{-1})	$J_0 \times 10^5$ (mmol/s.cm^2)	P*10^7 (cm^2 s^{-1})	$J_0 \times 10^5$ (mmol/s.cm^2)
25	0.0068	27.71	0.19	72.91	0.49
	0.0034	28.17	0.15	80.21	0.27
	0.0017	29.35	0.05	87.50	0.15
	0.0009	31.08	0.03	94.79	0.08
30	0.0068	28.35	0.21	73.56	0.52
	0.0034	29.81	0.17	81.64	0.28
	0.0017	30.73	0.06	88.01	0.16
	0.0009	32.46	0.04	95.37	0.09
35	0.0068	29.01	0.24	74.73	0.55
	0.0034	30.46	0.12	82.11	0.30
	0.0017	31.10	0.07	89.69	0.16
	0.0009	32.75	0.05	96.98	0.10

Table 3
Influence of temperature on the microscopic parameters of the facilitated transport of Cr (VI) ions.

	PIM(1)		PIM(2)	
T(°C)	D*10^5 cm^2.s^{-1}	K_{ass}	D*10^5 cm^2.s^{-1}	K_{ass}
25	20.24	3.26	29.83	7.09
30	21.82	2.99	32.50	5.80
35	25.11	2.60	45.52	2.12

4.5 Activation parameters

From the equation the transition state using the Arrhenius relation was applied for studying the variations of the fluxes, (J_0) means as a function of temperature.

The representations of $\ln J_0$ mean $=-E_a/R * (1/T) + \ln Aj$ (Equation 16), we obtained lines whose slope was ($-E_a/R$) and ordinated to the origins ($\ln Aj$). From the slopes and intercepts of these lines, the activation parameters (activation energy E_a, activation enthalpy $\Delta H^{\neq}$, and activation entropy $\Delta S^{\neq}$ related to the facilitated transport of Cr (VI)ions through the two studied membranes were calculated, and the results are presented in Table 4.

Table 4
Activation parameters related to the facilitated transport of Cr(VI) ions through the two membranes.

	PIM(1)	PIM(2)
Activation energy E_a (kJ.mol^{-1})	21.946	8,734
Activation entropy $\Delta S^{\neq}$ (J. mol^{-}.K^{-1})	-274.782	-311.951
Enthalpy of activation $\Delta H^{\neq}$ (kJ. mol^{-1}.K^{-1})	19.446	6.233

The values of the activation entropies corresponding to the transition state of the association/dissociation reaction of the substrate with the transporter were negative. This showed that in the transition state, there was a gain of order caused by a closer approach of the substrate and the transporter agent, indicative of an early transition state. For the two membranes studied, the values obtained for this parameter ($\Delta S^{\neq}$) were very close, which suggested that the association of the Cr (VI) ions with the transporter molecules during their passage through the two membranes occurred according to the same sites of interaction of the Gd-Glucaric acid transporter and the Cr (VI) substrate.

On the other hand, the low values of $\Delta H^{\neq}$ indicated low activation energy for these transition states in both membranes, and thus a rapid association/dissociation reaction (substrate-transporter). Therefore, the directed process of facilitated extraction of Cr (VI) ions across these two types of membranes was affected much more by the structural aspect than by the energetic aspect.

4.6 Effect of the presence of Ni (II) ions on the transport of Cr (VI)

The effect of the properties of the polymer support and the presence of Ni (II) ions was evaluated. The polymeric support in a polymer strongly affects the orientation process. It is related to the promotion of the extraction of metal ions through the PIM membrane. The simultaneous separation of Cr (VI) and Ni (II) ions using the two PIMs was investigated using different polymeric supports. The experiments were conducted under the following conditions: mixing the feed phase Cr (VI) = 0.0068M/0.0034M/0.0017M and 0.0009M and Ni (II)= 0.0251M/0.0125M/0.0063M and 0.0031 M ions, at pH = 3 and T = 25°C. The results are presented in Table 5.

The transport efficiencies of Cr (VI) and Ni (II) ions through the PIMs were strongly affected by the nature and structure of the PIM membranes. The results showed that using PVDF as a polymer can significantly improve the transport parameters (P and J_0) of Cr (VI) and Ni (II) by approximately 100% and 250%, respectively. Although the two ions were also co-transported into the receiving solution through the Gd-glucaric acid complex-based PIMs, a negligible change in the parameters (P and J_0) was observed. These results can be explained based on the electrostatic attraction between the two ions, which decreased the distribution of the ions on the surface of the membrane. The competition between the two ions at the active sites of the transporter also influenced the co-transport through the membranes.

Table 5
The comparison of the macroscopic parameters of two individual and simultaneous ions.

		Cr(VI)					Ni(II)			
		Cr(VI)Single		Cr(VI)_Simultaneous			Ni(II)Single		Ni(II)simultaneous	
T(°C)	C_0 (M)	P*10^7 (cm^2 s^{-1})	$J_0 \times 10^5$ (mmol/s.cm^2)	P*10^7 (cm^2 s^{-1})	$J_0 \times 10^5$ (mmol/s.cm^2)	C_0 (M)	P*10^7 (cm^2 s^{-1})	$J_0 \times 10^5$ (mmol/s.cm^2)	P*10^7 (cm^2 s^{-1})	$J_0 \times 10^5$ (mmol/s.cm^2)
PIM(1)	**0.0068**	27.71	0.19	18.23	0.12	**0.0251**	3.65	0.09	2.18	0.05
	0.0034	29.17	0.15	21.87	0.07	**0.0125**	7.12	0.08	3.64	0.04
	0.0017	31.35	0.05	25.52	0.04	**0.0063**	8.23	0.07	8.02	0.03
	0.0009	32.08	0.03	29.16	0.03	**0.0031**	9.45	0.04	6.56	0.02
PIM(2)	**0.0068**	72.91	0.49	73.64	0.50	**0.0251**	5.10	0.13	3.64	0.08
	0.0034	80.21	0.27	81.66	0.28	**0.0125**	7.29	0.11	4.37	0.05
	0.0017	87.50	0.15	89.68	0.16	**0.0063**	8.75	0.07	5.10	0.03
	0.0009	94.79	0.08	95.52	0.09	**0.0031**	10.94	0.06	5.83	0.02

5. Conclusion

In this study, a new extractive agent was designed to develop organic membranes. Subsequently, two membranes were characterized and tested in various process-oriented experiments of the facilitated extraction and recovery of Cr (VI) and Ni (II) ions from simulated wastewater. The values of the macroscopic and microscopic parameters associated with the processes (P, J_0, K_{ass}, and D*) were determined. These parameters were then used to analyze and quantify the performance of the adopted membranes as a function of factors such as the initial substrate concentration C_0, and temperature. Microscopic parameters (K_{ass} and D*) and activation parameters (E_a, $\Delta H^{\#,}$ and $\Delta S^{\#}$) were determined, analyzed, and correlated with the chemical structure of the membranes. The results were used to explain and confirm the performance of the membrane and elucidate the mechanism by which Cr (VI) ions jumped on fixed sites of the EA immobilized in the membrane phase. In the processes oriented for the extraction of Cr (VI) ions, the PIM prepared by the phase inversion method was observed to be more efficient compared to PSU. Using a PIM membrane allowed the co-extraction of Cr (VI) and Ni (II) ions from mixtures by the same mechanism based on the interactions between the substrate and the membrane, which explained the recorded selectivity.

The results of this study indicated that the developed PIM might be used for the selective extraction and separation of Cr (VI) ions from industrial liquid wastes. This type of stable polymeric membrane is used for the extraction and separation of other ions and dyes under different experimental conditions. They can be used to optimize the performance for the extraction and recovery of several ions and dyes from industrial wastes.

CRediT authorship contribution statement

Z. Habibi: Conceptualization, Data curation, Formal analysis, Writing – original draft.
Y. Chaouqi: Conceptualization, Data curation, Formal analysis, Writing – original draft.
M. Riri: Formal analysis.
S. Majid: Formal analysis.
Kh. Touaj: Writing – review & editing.
M. Hlaibi: Writing – review & editing.

Funding

This research did not receive any specific grant from funding agencies in the public, commercial, or not-for-profit sectors.

Declaration of Competing Interest

The authors declare that they have no known competing financial interests or personal relationships that could have appeared to influence the work reported in this paper.

Acknowledgments

The works in this manuscript are conducted within the framework of a PPR2 project, funded by the Ministry of Higher Education and Scientific Research (MESRSFC) and the National Center of Scientific and Technical Research (CNRST). We thank the leaders of these two organizations.

References

[1] A. Hasanbeigi and L, Price. A technical review of emerging technologies for energy and water efficiency and pollution reduction in the textile industry, J. Clean. Prod. 95 (2015) 30-44. https://doi: 10.1016/j.jclepro.2015.02.079.

[2] A.M. Elgarahy, K.Z. Elwakeel, S.H. Mohammad, and G.A. Elshoubaky. A critical review of biosorption of dyes.heavy metals and metalloids from wastewater as an efficient and green process. J. Clean. Prod. 4 (2021) 100209. https://doi: 10.1016/j.clet.2021.100209.

[3] N.A. Bakar, N. Othman, Z.M. Yunus, W.A.H. Altowayti, M. Tahir, N. Fitriani and S.N.A. Mohd-Salleh. An insight review of lignocellulosic materials as activated carbon precursor for textile wastewater treatment. Environ. Technol. Innov. 22 (2021) 101445. https://doi: 10.1016/j.eti.2021.101445.

[4] M.A. Al-kaabi, N. Zouari, D. Adel, and M.A. Al-ghouti. Adsorptive batch and biological treatments of produced water : Recent progresses, challenges, and potentials. J. Environ. Manage. 290 (2021) 112527. https://doi: 10.1016/j.jenvman.2021.112527..

[5] J.P. Vareda, A.J.M. Valente, and L. Durães. Ligands as copper and nickel ionophores: Applications and implications on wastewater treatment. Adv. Colloid Interface Sci. 89 (2021) 102364. https://doi: 10.1016/j.cis.2021.102364.

[6] M.S. Sankhla, R. Kumar, S.S. Sonone, and S. Jadhav. Water Contamination by Heavy Metals and their Toxic Effect on Aquaculture and Human Health through Food Chain. Letters in Applied NanoBioScience 10 (2021) 2148-2166. https://doi: 10.33263/LIANBS102.21482166.

[7] L. Bukman, N. R. C. Fernandes-Machado, W. Caetano, A. L. Tessaro, and N. Hioka. Treatment of wastewater contaminated with ionic dyes: Liquid-liquid extraction induced by reversed micelle followed by photodegradation. Sep. Purif. Technol. 189 (2017) 162-169. https://doi: 10.1016/j.seppur.2017.08.004.

[8] L.G.M. Silva, F.C. Moreira, M.A.P. Cechinel, L.P. Mazur, A.A. Ulson de Souza, S.M.A. Guelli U. Souza, R.A.R. Boaventura, V.J.P. Vilar. Integration of Fenton's reaction-based processes and cation exchange processes in textile wastewater treatment as a strategy for water reuse. J. Environ. Manage. 272 (2020) 111082. https://doi: 10.1016/j.jenvman.2020.111082.

[9] F. Minas, B.S. Chandravanshi, S. Leta, Chemical precipitation method for chromium removal and its recovery from tannery wastewater in Ethiopia. Chem. Int. 3 (2017) 291-305. https://doi: 10.31221/osf.io/m7h5k..2017.392-405

[10] L. Yang, W. Hu Zhang, T. Liu, D. Fang, P. Shao, H. Shi, X. Luo. Electrochemical recovery and high value-added reutilization of heavy metal ions from wastewater: Recent advances and future trends. Environ. Int. 152 (2021) 106512. https://doi: 10.1016/j.envint.2021.106512.

[11] Y. Chaouqi, R. Ouchn, I. Touarssi, I. Mourtah, M. EL Bouchti, L. Lebrun, O. Cherkaoui and M. Hlaibi. Polymer Inclusion Membranes for Selective Extraction and Recovery of Hexavalent Chromium Ions from Mixtures Containing Industrial Blue P3R Dye. Ind. Eng. Chem. Res. 58 (2019) 18798-18809. https://doi: 10.1021/acs.iecr.9b03026.

[12] Y. Chaouqi, M. El Bouchti, R. Ouchn, Z. Habibi, O. Cherkaoui, and M. Hlaibi. Oriented membranes processes for facilitated extraction and recovery of some industrial dyes across polymer inclusion membranes containing Chitin as new extractive agent. IOP Conference Series: Mater. Sci. Eng. 827 (2020) 1. https://doi: 10.1088/1757-899X/827/1/012001.

[13] J. López, O. Gibert, and J. L. Cortina. Integration of membrane technologies to enhance the sustainability in the treatment of metal-containing acidic liquid wastes. An overview, Sep. Purif. Technol. 265 (2021). https://doi: 10.1016/j.seppur.2021.118485.

[14] E.H. El Atmani, A. Benelyamani, H. Mouadili, S. Tarhouchi, S. Majid, K. Touaj, L. Lebrun and M. Hlaibi.The oriented processes for extraction and recovery of paracetamol compound across different affinity polymer membranes. Parameters and mechanisms, Eur. J. Pharm. Biopharm. 126 (2018) 201-210. https://doi: 10.1016/j.ejpb.2017.06.001.

[15] Y.S. Dzyazko, V.M. Linkov, and V. N. Belyakov, Electrical conductivity of a flexible resin loaded with Cr(III) ions. Desalination 241 (2009) 57-67. https://doi: 10.1016/j.desal.2007.10.099.

[16] D. Vasanth, G. Pugazhenthi, and R. Uppaluri. Biomass-assisted microfiltration of chromium(VI) using Baker's yeast by ceramic membrane prepared from low-cost raw materials. Desalination 285 (2012) 239-244. https://doi:10.1016/j.desal.2011.09.055.

[17] A. Benjjar, T. Eljaddi, O. Kamal, K. Touaj, L. Lebrun, and M. Hlaibi. The development of new supported liquid membranes (SLMs) with agents: Methyl cholate and resorcinarene as carriers for the removal of dichromate ions ($Cr_2O_7^{2-}$). J. Environ. Chem. Eng. 2 (2014) 503-509. https://doi: 10.1016/j.jece.2013.10.003.

[18] M. Muthukrishnan and B.K. Guha. Effect of pH on rejection of hexavalent chromium by nanofiltration. Desalination 219 (2008) 171-178. https://doi: 10.1016/j.desal.2007.04.054.

[19] M. Chiha, M. H. Samar, and O. Hamdaoui. Extraction of chromium (VI) from sulphuric acid aqueous solutions by a liquid surfactant membrane (LSM). Desalination 194 (2006) 69-80. https://doi: 10.1016/j.desal.2005.10.025.

[20] A. Kaya, C. Onac, H. K. Alpoguz, A. Yilmaz, and N. Atar. Removal of Cr(VI) through calixarene-based polymer inclusion membrane from chrome plating bath water. Chem. Eng. Res. Des. 283 (2016) 141-149. https://doi: 10.1016/j.cej.2015.07.052.

[21] L. Guo, Y. Liu, C. Zhang, and J. Chen. Preparation of PVDF-based polymer inclusion membrane using ionic liquid plasticizer and Cyphos IL 104 carrier for Cr(VI) transport. J. Membr. Sci. 372 (2011) 314-321. https://doi: 10.1016/j.memsci.2011.02.014.

[22] Y. Chaouqi, R. Ouchn, T. Eljaddi, A. Jada, M. El Bouchti, O. Cherkaoui and M Hlaibi .New polymer inclusion membrane containing NTA as carrier for the recovery of chromium and nickel from textiles wastewater. Mater. Today Proc. 13 (2019) 698-705. https://doi: 10.1016/j.matpr.2019.04.030.

[23] M. Riri, M. Hor, F. Serdaoui, and M. Hlaibi. Complexation of trivalent lanthanide cations by different chelation sites of malic and tartaric acid (composition, stability and probable structure). Arabian Journal of Chemistry, 9 (2016) 1478–1486. https://doi.org/10.1016/j.arabjc.2012.03.012.

[24] M. Hlaïbi, N. Tbeur, A. Benjjar, O. Kamal, and L. Lebrun. Carbohydrate-resorcinarene complexes involved in the facilitated transport of alditols across a supported liquid membrane. J. Membr. Sci. 377 (2011) 231-240. https://doi: 10.1016/j.memsci.2011.04.055.

[25] K. Touaj, N. Tbeur, M. Hor, J. F. Verchère, and M. Hlaïbi. A supported liquid membrane (SLM) with resorcinarene for facilitated transport of methyl glycopyranosides: Parameters and mechanism relating to the transport, J. Membr. Sci. 337 (2009) 28-38. https://doi: 10.1016/j.memsci.2009.03.014.

[26] T. Eljaddi, M. Hor, A. Benjjar, M. Riri, H. Mouadili, Y. Mountassir, and M. Hlaibi, New Supported Liquid Membrane for Studying Facilitated Transport of U(VI) Ions Using Tributyl Phosphate (TBP) and Tri-n-Octylamine (TOA) as Carriers from Acid Medium. BAOJ Chem. 1 (2015). https://doi: 10.24947/baojc/1/1/103.

[27] R. Louafy, A. Benelyamani, S. Tarhouchi, O. Kamal, K. Touaj, and M. Hlaibi Parameters and mechanism of membrane-oriented processes for the facilitated extraction and recovery of norfloxacin active compound. Environ. Sci. Pollut. Res. 27 (2020) 37572-3758. https://doi: 10.1007/s11356-020-09311-0.

[28] H. Eyring, The activated complex in chemical reactions. J. Chem. Phys. 3 (1935) 63-71. https://doi: 10.1063/1.1749604.

[29] M. Hor, A. Riad, A. Benjjar, L. Lebrun, M. Hlaïbi, Technique of supported liquid membranes (SLMs) for the facilitated transport of vanadium ions (VO2+): Parameters and mechanisms on the transport process, Desalination 255 (2010) 188-195. https://doi: 10.1016/j.desal.2009.12.023.

[30] O. Kamal, T. Eljaddi, El H. El Atmani, I. Touarssi, I. Mourtah, L. Lebrun, and M. Hlaibi. Process of Facilitated Extraction of Vanadium Ions through Supported Liquid Membranes: Parameters and Mechanism. Adv. Mater. Sci. Eng. 2017 (2017) 3425419. https://doi: 10.1155/2017/3425419.

[31] S. Tarhouchi, R. Louafy, E. Houssine, E. L. Atmani, and M. Hlaïbi, Kinetic control concept for the diffusion processes of Paracetamol active molecules across affinity polymer membranes. BMC Chem. Biol. 16 (2022) 2. https://doi.org/10.1186/s13065-021-00794-7.